Gene induction by glycyrol to apoptosis through endonuclease G in tumor cells and prediction of oncogene function by microarray analysis

SungGa Lee[a,d], Hyun-Mee Oh[d], Won-Bong Lim[a], Eun-Ju Choi[d], Young-Na Park[d], Jeong-Ah Kim[e], Ji-Young Choi[e], Suk-Jin Hong[c], Hee-Kyun Oh[b], Jong-Keun Son[e], Seung-Ho Lee[e], Ok-joon Kim[a], Hong-ran Choi[a] and Chang-Duk Jun[d]

Glycyrrhiza uralensis **(Leguminosae) has long been known as an antiinflammatory agent for gastric ulcers, arthritis, and rheumatism. The flavonoid glycyrol (GC) (10 μg/ml) isolated from *G. uralensis* dramatically inhibits phorbol ester (phorbol 12-myristate 13-acetate)-induced nuclear factor (NF)-κB-dependent transcriptional activity, as determined by luciferase reporter activity in human kidney epithelial 293T cells. To investigate global gene expression profiling in cells by GC, we performed high-density oligonucleotide microarrays. Our microarray analyses showed that GC inhibited phorbol ester-induced NF-κB-dependent transcriptional activity in inflammatory-related gene expression. RT-PCR analysis, based on microarray data, showed that NF-κB-dependent genes (such as CCL2, CCL7, CD44, and HSPB8 in addition to NF-κB itself) were significantly downregulated by GC. Treatment with GC (10 μg/ml) inhibited I-κB degradation induced by phorbol 12-myristate 13-acetate. The microarray data also suggested that GC induces gene expression to p53-dependent apoptosis through endonuclease G, instead of CAD/DFF and AIF/PDCD8, as a downstream-apoptosis factor in human kidney epithelial 293T tumor cells, and induces oncogenes with a suppressor role as an added function.** ***Anti-Cancer Drugs*** **19:503–515 © 2008 Wolters Kluwer Health | Lippincott Williams & Wilkins.**

Anti-Cancer Drugs 2008, **19**:503–515

Keywords: apoptosis, endonuclease G, glycyrol, human kidney epithelial 293T, inflammation, microarray, oncogenesis, p53

[a]Department of Oral Pathology, 2nd Stage of Brain Korea 21 for School of Dentistry, Dental Science Research Institute, Departments of [b]Oral Maxillofacial Surgery, [c]Preventive and Public Health Dentistry, School of Dentistry, Chonnam National University, [d]Department of Life Science, Gwangju Institute of Science and Technology, Gwangju and [e]College of Pharmacy, Youngnam University, Gyeongsan, Korea

Correspondence to Dr Chang-Duk Jun, Department of Life Science, Gwangju Institute of Science and Technology, Gwangju 500-712, Korea
Tel: +82 62 970 2506; fax: +82 62 970 2546;
e-mail: cdjun@gist.ac.kr

Received 13 September 2007 **Revised form accepted** 5 February 2008

Introduction

Traditional medicines have attracted considerable interest in view of their many claimed benefits, which include antidiabetic, antimicrobial, antiviral, antiinflammatory, and antiallergic activities, as well as anticancer effects. *Glycyrrhiza uralensis* is one of the oldest herbal medicines known and has been the subject of extensive studies. Some components of *G. uralensis*, specifically glycyrrhizin and licocoumarone, exhibit pharmacological effects on conditions such as inflammation, ulcer, allergy, and carcinogenesis. In addition, a water or ethanol extract of *Glycyrrhiza* is known to reduce experimentally induced cognitive deficits, gastric ulcer, arthritis, and rheumatism. There has been, however, little investigation of glycyrol (GC), another component of *G. uralensis*, in terms of its effect on inflammation, apoptosis, and oncogenesis.

Several reports have indicated that exploring the ability to selectively inhibit nuclear factor (NF)-κB transcription factors could be useful in developing drugs with therapeutic applications in treating diseases involving inflammation, apoptosis, and oncogenesis [1–3]. In fact, many small molecular NF-κB inhibitors, such as glucocorticoids, antioxidants, and proteasome inhibitors, have been reported, albeit some of these have pleiotropic effects on various other cell functions and cause unfavorable side effects when used therapeutically.

In this study, we screened five single compounds, purified from *G. uralensis*, to determine their ability to attenuate phorbol ester-induced NF-κB activity in human kidney epithelial (HEK)-293T cells. Of these, we found that flavonoid GC (10 μg/ml) dramatically inhibits phorbol ester [phorbol 12-myristate 13-acetate (PMA)]-induced NF-κB-dependent luciferase activity in HEK293T cells. Many flavonoids also show potent antitumor activity, through induction of p53-dependent apoptosis and cell cycle arrest in several cancer cell lines [4–7]. To explore the global effect of GC in phorbol ester-induced cellular activation, we used DNA microarrays. This allowed us to examine the global gene expression pattern in HEK293T tumor cells. Meanwhile, biochem-

ical and genetic studies also identified at least three nucleases for end-stage DNA fragmentation during cell death: CAD/DFF (caspase-activating DNase), AIF/PDCD8 (apoptosis-inducing factor/programmed cell death 8), and endonuclease G (ENDO G). In this study, we found changes in gene expression in the tumor cells, causing apoptosis through ENDO G, instead of through CAD/DFF and AIF/PDCD8 as the downstream-apoptosis factor, and also causing a potential suppression of oncogenesis in HEK293T tumor cells, in response to PMA in the presence of GC.

Materials and methods

Reagents and antibodies

PMA, dimethyl sulfoxide, phosphate-buffered saline (PBS), and 3-(4, 5-dimethylthiazol-2-yl)-2, 5-diphenyltetrazolium bromide (MTT) were supplied by Sigma Chemical Co. (St Louis, Missouri, USA). Horseradish peroxidase-conjugated antirabbit immunoglobulin G was supplied by Amersham Biosciences UK (Little Chalfont, England, UK). Antihuman I-κBα was obtained from Santa Cruz Biotechnology (Santa Cruz, California, USA).

Cell culture

HEK 293T cells were obtained from the American Type Culture Collection. The cells were cultured at 37°C in a 5% CO_2 atmosphere in RPMI 1640, supplemented with heat-inactivated 10% fetal bovine serum (GibcoBRL, Karlsruhe, Germany) and appropriate antibiotics.

Plant material

The roots of *G. uralensis* (Leguminosae) were purchased at Yangnyeongsi, Daegu, South Korea, in November 1999 and identified by Professor Je-Hyun Lee, College of Oriental Medicine, Dongguk University, Gyeonju, South Korea. A specimen has been deposited at the College of Pharmacy, Yeunnam University, South Korea.

Isolation of compounds from *G. uralensis*

Compounds were extracted from the roots of *G. uralensis* (10 kg) with methanol (50 l) at room temperature. The methanol extract was evaporated under reduced pressure to obtain a residue (2.6 kg), which was dissolved in water (3.5 l) and partitioned with methylene chloride (3.5 l × 3). The methylene chloride-soluble fraction (230 g) was chromatographed on silica gel (6.2 kg), and eluted with *n*-hexane, with the polarity gradually increased with ethyl acetate (100 : 0, 98 : 2, 95 : 5, 90 : 10, 85 : 15, 80 : 20, 5 l for each gradient), to give 16 fractions (fractions 1–16). Of these, fraction 4 (3200 ml, *n*-hexane-ethyl acetate, 98 : 2) and fraction 8 (1200 ml, *n*-hexane-ethyl acetate, 90 : 10) were both crystallized from cold methanol to yield GC (450 mg, 90% of purity), which was purified by preparative high-performance liquid chromatogram (25 mm i.d. × 350 mm, shimpack Pre-ODS column; Shimadzu, Japan) with elution by MeOH:H_2O [70 : 30 (v/v), 7 ml/min] to afford pure GC (110 mg, 99% of purity) [8]. Fraction 9 (2400 ml, *n*-hexane-ethyl acetate, 90 : 10) was rechromatographed over silica gel (300 g), eluting with methylenechloride:MeOH (1.5 l) to give liquiritigenin (300 mg, 100% of purity) [9]. Fraction 12 (3600 ml, *n*-hexane-ethyl acetate, 80 : 20) was chromatographed over silica gel (700 g), eluted with methylenechloride:MeOH (95 : 5, 2 l) to give glycyrrhizin (950 mg, 98% of purity) and ononin (70 mg, 92% of purity). Further preparative high-performance liquid chromatography (25 mm i.d. × 350 mm, shimpack Prep-ODS column; Shimadzu) with elution by MeOH:H_2O [50 : 50 (v/v), 7 ml/min] yielded pure ononin (10 mg, 99% of purity) [10,11]. Ammonium glycyrrhizinate was prepared according to Kondratenkos's method [12–14]. An acetone solution (10 ml) of glycyrrhizin (800 mg) was gradually added with stirring to a 25% NH_4OH solution to pH approximately 8–8.5. The reaction mixture was filtered and washed with ethanol, and dried in air to obtain 600 mg of reaction product. This reaction product was treated by heating with 3 ml of glacial AcOH, washed with ethanol, and recrystallized from an 85% ethanol to obtain pure ammonium glycyrrhizinate (520 mg, 99% of purity). Carbenoxolone disodium salt was manufactured using 23.5 g of glycyrrhetinic acid, which were dissolved in 50 ml of dry pyridine. A solution of 6.0 g of succinic anhydride in 30 ml of dry pyridine was added, followed by 30 ml of dry triethylamine and then, for washing purposes, 5 ml of dry pyridine. The solution was heated in a bath of boiling water for 10 h, and then poured into a container of dilute hydrochloric acid and ice. The fine gray precipitate thus produced was filtered off, washed with water, dissolved in chloroform, and the solution extracted repeatedly with dilute hydrochloric acid and later with water. It was dried over sodium sulfate and evaporated. Crystallization from methanol, using charcoal to effect decolorization, produced carbenoxolone as cream-colored crystals, melting point of 291–294°C, with previous softening. A preparation with one molecular proportion of carbenoxolone was ground with a dilute aqueous solution (5%) containing two molecular proportions of sodium hydroxide. The solution was filtered and evaporated in vacuum over concentrated sulfuric acid. Carbenoxolone disodium salt (99% of purity) was thereby obtained as a creamy white water-soluble solid [15]. The chemical structures were identified by comparison of spectral data and their hydrolysates with those published previously [8–11,15]; these structures are represented in Fig. 1a.

Cell extract preparation and western blot analysis

The HEK293T cells were cultured for 12 h after being seeded at 1×10^5 cells per 12-well plate. The culture media were exchanged 1 h before reagent treatment, and the cells were pretreated with components (10 μg/ml) extracted from *G. uralensis* for 30 min, and then were further incubated for 4–48 h with PMA (100 nmol/l) at 37°C. For the analysis of total protein levels in the I-κB degradation, stimulated cells were rinsed twice with ice-

Fig. 1

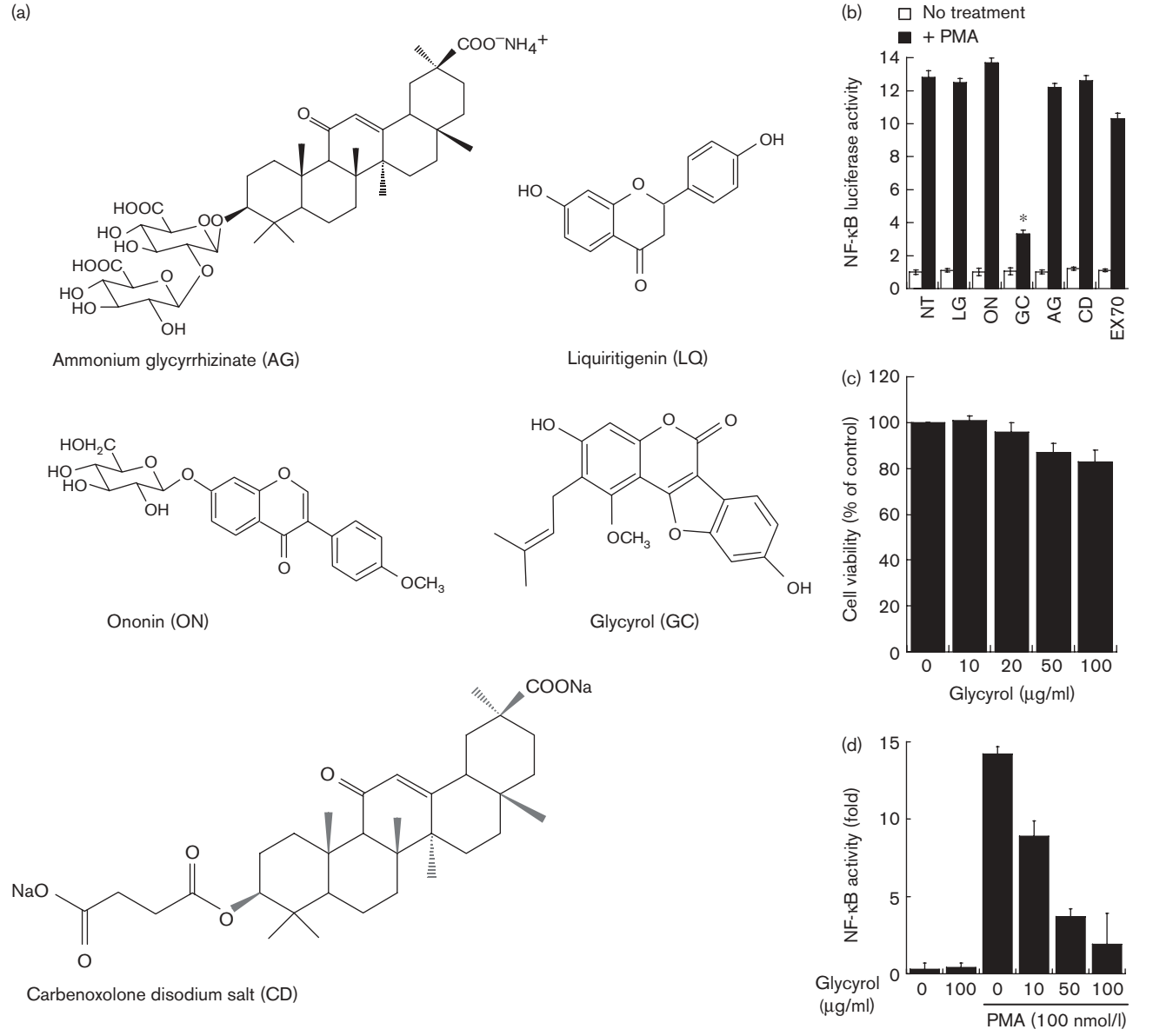

Chemical structures and determination of glycyrol by nuclear factor (NF)-κB promoter activity assay. (a) Chemical structures of compounds isolated from *Glycyrrhiza uralensis*, which have a purity of 99% by high-performance liquid chromatography. (b) HEK293T cells (1×10^5) were transfected with NF-κB luciferase reporter vector (0.8 μg/well). Cells were pretreated with components (10 μg/ml) for 30 min and then were further incubated for 16 h with phorbol 12-myristate 13-acetate (PMA) (100 nmol/l). The relative luciferase activity was measured using the Luciferase Assay System. AG, ammonium glycyrrizinate; CD, carbenoxolone disodium salt; EX70; 70% ethanol extract of *G. uralensis*; GC, glycyrol; LG, liquiritigenin; NT, not treated; ON, ononin. *Glycyrol inhibits the promoter activity of NF-κB induced by PMA. (c) HEK293T cells (1×10^5) were treated with various concentrations of glycyrol (0-100 μg/ml) for 24 h. These data are representative of three independent experiments. (d) Cells (5×10^5) were pretreated with various concentrations of glycyrol (0-100 μg/ml) for 30 min and then the cells were further incubated for 24 h with PMA (100 nmol/l). NF-κB protein levels were determined by enzyme-linked immunosorbent assay.

cold PBS and then lysed in ice-cold lysis buffer [50 mmol/l Tris–HCl, pH 7.4, containing 150 mmol/l NaCl, 1% Nonidet P-40 (cat. no. 23640-94; Nacalai Tesque; Kyoto, Japan), 0.1% SDS, 0.1% deoxycholate, 5 mmol/l sodium fluoride, 1 mmol/l sodium orthovanadate, 1 mmol/l 4-nitrophenylphosphate, 10 g/ml leupeptin, 10 mg/ml pepstatin A, and 1 mmol/l 4-(2 aminoethyl) benzenee sufonyl fluoride]. Cell lysates were centrifuged at 15 000*g* for 20 min at 4°C. The supernatant was mixed with a one-fourth volume of 4 × SDS sample buffer, boiled for 5 min, and then separated through a 12% SDS–PAGE gel. After electrophoresis, the proteins were transferred to a nylon membrane by means of Trans-Blot SD semi-dry transfer (Bio-Rad, Hercules, California, USA). The membrane

was blocked in 5% skim milk for 1 h, rinsed, and incubated with the primary antibody for I-κB in Tris-buffered saline (TBS) containing 0.05% Tween 20 (TBS-$T_{0.05}$) including 3% skim milk overnight at 4°C. Afterwards the membrane was washed four times in TBS containing 0.05% Tween 20, and the membrane was incubated with 0.1 mg/ml peroxidase-labeled secondary antibody for 1 h. After three washes in TBS Tween 20, the membrane was exposed to radiograph with ECL Western Blotting Detection reagents (Amersham Pharmacia, Piscataway, New Jersey, USA).

Nuclear factor-κB luciferase reporter gene assay

HEK293T cells were seeded at 5×10^5 in a 12-well plate 1 day earlier transient transfection (90–95% cell confluency). Cells were transfected with 1.6 μg/ml NF-κB luciferase reporter construct in serum-free and antibiotic-free RPMI 1640 medium containing Lipofectamine 2000 reagent (Invitrogen, Carlsbad, California, USA). After 5 h of incubation, the medium was replaced with fresh RPMI 1640 medium containing 10% fetal bovine serum and antibiotics. After 24 h of transfection, cell extracts were prepared and the relative luciferase activity was measured using the Luciferase Assay System (Promega, Madison, Wisconsin, USA), according to the manufacturer's instructions.

Cell viability assay

Cellular viability was evaluated by the reduction of MTT to formazan. A stock solution of MTT was prepared in PBS, diluted in RPMI 1640 medium, and added to the cell-containing wells at a concentration of 0.5 mg/ml after the culture medium was first removed. The plates were then incubated for 4 h at 37°C in 5% CO_2. At the end of the incubation period, the medium was aspirated, and the formazan product was solubilized with dimethyl sulfoxide. Absorbency was measured on a multiscan reader with a 570-nm wavelength filter.

RNA isolation

HEK293T cells (3×10^6) were grown in a 60-mm culture dish for 12 h and were then incubated for 24 h in a fresh medium containing GC (10 μg/ml), PMA (200 nmol/l), or GC and PMA, as mentioned above. Cells were harvested and total RNA was isolated using easy Blue (iNtRON Biotechnology, Korea) according to the manufacturer's instructions. Total RNA samples were measured for quality at 260/280 nm, 260/230 nm, and using the 28S/18S ratio. The quality was further confirmed by agarose gel electrophoresis.

Complementary DNA preparation and microarray hybridization

For each hybridization, 2-deoxyuridine 5-triphosphate-labeled complementary DNA (cDNA) was amplified from the total RNA samples (5 μg per sample) by RT-IVT Labeling Reagents (Applied Biosystems, California, USA). An approximately 50-μg labeled cDNA sample was subsequently purified using RT-IVT Purification Components (Applied Biosystems). The resulting samples were hybridized on a microarray chip containing 33 096 oligonucleotide clones (Applied Biosystems) and further processed according to the Applied Biosystems protocol.

Oligonucleotide microarray analysis

Microarray images were acquired with an AB 1700 microarray analyzer (Applied Biosystems). Signal quantification and data processing were performed using AVADIS (Strand Genomics, Bangalore, India). Each experiment was repeated three times to reduce the risk of false-positive or false-negative results. The results from the three independent identical experiments were then merged and the merged data were used for subsequent comparisons. The average intensity values of signal for each gene were calculated. Significant differences in gene expression between untreated and treated cells were determined using the analysis of variance test and the *t*-test with a significance threshold of *P* value less than 0.05. To estimate fold induction, the ratios of treated to untreated signal intensities were calculated. The $\log_2$ of each ratio was determined to equalize the magnitude of deflection in upregulated and downregulated genes, and gene expression differences were ranked based on absolute values.

RT-PCR

Seven genes, differentially expressed in microarray experiments, were selected for RT-PCR experiments to validate the induction levels measured. Each set of samples was analyzed in triplicate. The RNA samples used in the RT-PCR experiments were identical to those used in the microarray experiments. Reverse transcription of the RNA was performed using the RT PreMix Kit (iNtRON). RNA (1 μg) and the primers (100 pmol) were preincubated at 70°C for 5 min and transferred to a mixture tube. The reaction volume was 20 μl. cDNA synthesis was performed at 42°C for 60 min, followed by RT inactivation at 94°C for 5 min. Thereafter, the RT-generated cDNA (2–5 μl) was amplified using the PCR PreMix Kit (iNtRON). The primers used for cDNA amplification were: 5′-CAAGATGACCAAGATGTATAAA GG-3′ (sense) and: 5′-AACAGTGTAGGTCTTGGTGA AG-3′ (antisense) for TIMP1; 5′-ATGGCTGACGGTC AGATGCCCTT-3′ (sense) and 5′-GTTGTTGAAACT GCTCTCTCCAAAT-3′ (antisense) for HSPB8; 5′-TG AGCAATAGCCTGCCATGTT-3′ (sense) and 5′-AATAG GTGACAGCCCGGCCAGAGT-3′ (antisense) for NF-κB1; 5′-TACTTCAACTACCTGCTGCTACAGA-3′ (sense) and 5′-GTTTTCTTGTCCAGGTGCTTCATA-3′ (antisense) for CCL7; 5′-AATGGTCGCTACAGCATCTC-3′ (sense) and 5′-TGTCTTCAGGATTCGTTCTG-3′ (antisense) for CD44; 5′-TGTGCCTGCTGCTCATAG CAG-3′ (sense) and 5′-TGGAATCCTGAACCCACTT CTG-3′ (antisense) for CCL2; 5′-CGGAGTCAACG

GATTTGGTCGTAT-3′ (sense) and 5′-AGCTTCTCCA TGGTGGTGAAGAC-3′ (antisense) for glyceraldehyde-3-phosphate dehydrogenase. PCR conditions were 94°C for 30 s in the denaturation step, 56°C for 30 s in the annealing step, and 72°C for 30 s in the extension step for 30 cycles. The expected PCR products were 247 bp (for TIMP1), 552 bp (for HSPB8), 340 bp (for NF-κB1), 350 bp (for CCL7), 388 bp (for CD44), 237 bp (for CCL2), and 306 bp (for glyceraldehyde-3-phosphate dehydrogenase).

Results

Glycyrol inhibited phorbol 12-myristate 13-acetate-induced nuclear factor-κB-dependent transcriptional activity in HEK293T cells

To study whether changes in gene expression by GC are NF-κB-dependent, we examined whether GC inhibits NF-κB-dependent transcriptional activity in PMA-treated HEK293T cells by measuring luciferase reporter activity. As shown in Fig. 1b, incubation of HEK293T cells with GC (10 μg/ml) significantly decreased PMA-induced luciferase activity. Cells (5×10^5) were pretreated with GC for 30 min, and were then incubated for a further 16 h with PMA (100 nmol/l). HEK293T cells (1×10^5) were treated with GC (10 mg/ml) and PMA (100 nmol/l) for 0, 4, 8, 16, 24, 36, and 48 h. Twenty-four hours was selected as the most appropriate exposure time for the cells because their incubation with GC and PMA for this period significantly decreased PMA-induced luciferase activity: there was no point in using greater exposure times (data not shown). To effectively test whether GC affects the viability of HEK293T cells, we performed a MTT assay (Fig. 1c). Concentrations ranging from 0 to 20 μg/ml of GC showed no toxic effects on HEK293T cells after 24 h of incubation, whereas higher concentrations of GC (> 50 μg/ml) induced cytotoxicity after 24 h. Flavonoids, including GC, are widely distributed in plants. Their relatively low toxicity compared with other active plant compounds means that humans and many other animals ingest significant quantities in their diet. An NF-κB activity analysis revealed that GC (0–20 μg/ml) significantly inhibited PMA (100 nmol/l)-dependent expression of luciferase mRNA in HEK293T cells (Fig. 1d). One hundred micrograms per milliliter of GC dramatically decreased PMA-induced NF-κB expression in a dose-dependent manner. As this concentration was, however, cytotoxic after 24 h of treatment (Fig. 1c), we used 10 μg/ml of GC for our experiments.

Gene expression analysis using DNA microarrays

Earlier studies indicate that extracts from *Glycyrrhiza* species can produce several pharmacological effects, including reduction of inflammation, ulcer, allergies, and carcinogenesis. It is not clear which compounds have these specific effects. This study, however, uses oligonucleotide microarrays with high quality total RNA samples (OD at 260/280 nm $\geq$ 1.9, OD at 260/230 nm > 1.7, and 28S/18S ratio = about 2 : 1) from HEK293T cells stimulated with single components of a *Glycyrrhiza* extract to provide additional information.

We carried out gene expression profiling after the DNA microarray and then assessed the molecular phenotype of genes expressed in HEK293T cells treated with the *Glycyrrhiz*-extracted GC (10 μg/ml). Total RNA was collected from three independent PMA-treated or GC-treated cell samples; labeled complementary RNA was hybridized to individual oligonucleotide chips, and the gene expression profile of each sample was determined using the AB 1700 microarray analyzer and AVADIS program. Of the 33 096 transcripts interrogated on the DNA chips, 12 556 (approximately 38% of the genome, flag value < 5000, SN > 3) and then 1322 (approximately 4% of the genome, *P* value < 0.05) transcripts were filtered, successively (Fig. 2a). To screen inflammatory-related, apoptosis-related, and oncogenesis-related genes for functional analysis of genes, the internal Panther or GO (Gene Ontology) function in AVADIS was used. When the gene expression profiles were compared, 789 genes [approximately 2.4% of the genome, FC of PMA to control (FC) > 1.5] had a statistically significant difference in terms of mRNA abundance in PMA-treated cells, compared with that in control cells, which had not been treated with GC or PMA. Importantly, the gene expression was then remodulated in PMA-treated cells by pretreatment of GC (Fig. 2b).

When the 789 genes were organized into expression categories, four sets (set 1, 257 rows; set 2, 135 rows; set 3, 323 rows; set 4, 74 rows) were made by Profile clustering in AVADIS (Fig. 2c). Set 1 genes exhibited upregulation by PMA and then were recovered from the upregulation by GC. Set 2 was a gene group upregulated by PMA and then further upregulated by GC. Set 3 showed a gene group downregulated by PMA and then recovered from downregulation by GC. Set 4 was a gene group downregulated by PMA and then further downregulated by GC.

Glycyrol modulation of phorbol 12-myristate 13-acetate-induced inflammation-related genes to inhibit inflammation through nuclear factor-κB-dependent pathways

From the genes in the four sets (789 genes) shown in Fig. 2c and described above, each functional group was annotated (shown in Fig. 3a). The group of Immunity and Defense (set 1, 61.1%; set 2, 27.8%; set 3, 11.1%; set 4, 0%) showed noticeable gene expression in set 1 (asterisk) (Fig. 3a, Table 1). The NF-κB gene (FC > 3) was found in set 1 of the group of Immunity and Defense based on the *t*-test analysis of AVADIS (Fig. 3a and b, Table 1). This result was consistent with the result shown in Fig. 1b for the NF-κB promoter reporter assay in PMA-stimulated HEK293T cells induced by GC.

Fig. 2

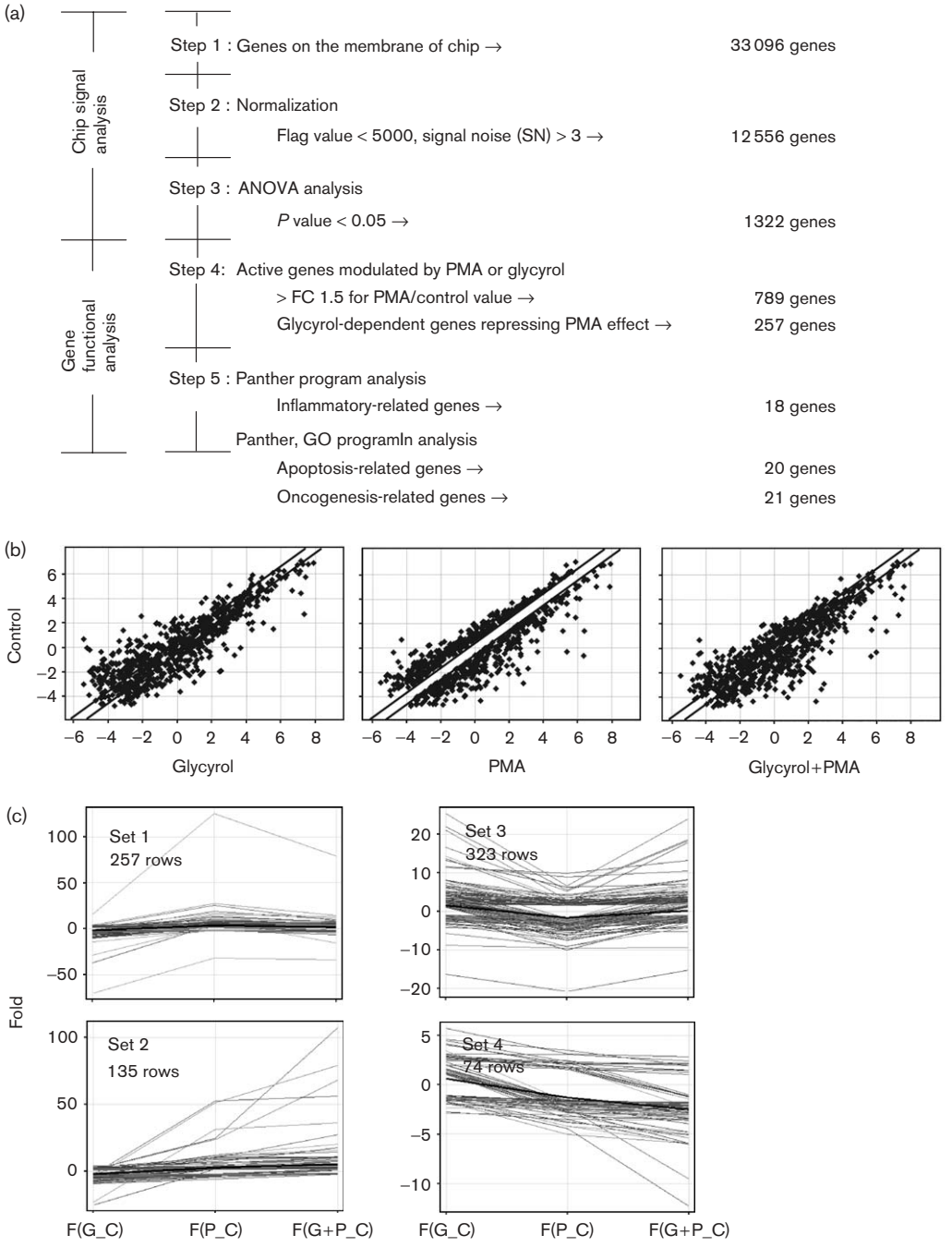

DNA chip array and profile clustering analysis of gene expression. These results were obtained from three independent experiments on microarray chips. (a) Gene scan procedure within each chip signal and two functional program analyses. (b) Clustering plots presenting glycyrol-dependent genes induced by phorbol 12-myristate 13-acetate (PMA). Seven hundred and eighty-nine genes with the normalized fluorescence intensity for each group were plotted with analysis of variance. The signal intensity for each gene in normal HEK293T cells was plotted against the signal intensity for each gene in HEK293T cells treated with glycyrol (10 μg/ml), PMA, and glycyrol and PMA, respectively. The solid diagonal lines indicate 1.5-fold increased or decreased fluorescence intensity. (c) A total of 789 genes were clustered based on their expression profiles. Genes with similar expression patterns are clustered together as the graphic representation. Sets 1, 2, 3, and 4 show expression of genes with up–down, up–up, down–up, and down–down pattern by PMA and glycyrol plus PMA, respectively. The thick black line within each cluster is an average expression profile of genes. F(G_C), fold (glycyrol/control); F(P_C), fold (PMA/control); F(G + P_C), fold (glycyrol + PMA/control).

The inflammation-related genes, CCL2, CCL7, HSPB8, and CD44 (four genes are in set 1 of the group of Immunity and Defense, FC > 3), as well as the NF-κB gene, were assessed by RT-PCR, and these results were in agreement with those of the *t*-test from AVADIS (Fig. 3a and b, Table 1). A Western blot analysis for I-κBα degradation within cells after treatment with GC (10 μg/ml), PMA, or a combination of the two, showed that I-κBα degradation was GC dependent (Fig. 3c). These results indicate that GC modulates PMA-induced inflammation-related genes to inhibit NF-κB-dependent pathways.

Glycyrol appears to induce gene expression related to p53-dependent apoptosis through ENDO G, instead of through CAD/DFF and AIF/PDCD8, as the downstream-apoptosis factor in HEK293T tumor cells, and to induce oncogenes with suppression function as an added role

An RT-PCR result confirmed that genes related to inhibition of apoptosis such as TIMP1 (tissue inhibitor of metalloproteinase 1, FC > 3) [16] are modulated by GC. This was confirmed by the result of the AVADIS *t*-test (Fig. 3d), which was carried out anticipating that GC may modulate gene expression to induce apoptosis in HEK293T tumor cells. We investigated the expression pattern for apoptosis-related genes in 789 genes (FC > 1.5, Fig. 2a) using the Panther or GO function. Surprisingly, apoptosis-related genes in 789 genes were involved in the induction of GC-modulated apoptosis in tumor cells (sets 2 and 3 in Table 2). Meanwhile, our microarray data showed that p53 (tumor protein p53), BID (BH3-interacting domain death agonist), and granzyme (GZM)-M were upregulated, but that CASPs (caspase 3, 6, and 7) were also downregulated by GC (Fig. 4a and b). Among downstream-apoptosis factors, CAD/DFF B, and AIF/PDCD8 (programmed cell death 8) were downregulated, but ENDO G was upregulated by GC (Fig. 4b and c). Galectin (GAL)-1 were upregulated, but GAL3, GAL9, and TRAP1 (tumor necrosis factor type 1 receptor associated protein) were downregulated by GC (Fig. 4d). Overall, GC seems to induce gene expression related to p53-dependent apoptosis through ENDO G instead of CAD/DFF and AIF/PDCD8 as downstream apoptosis factor in HEK293T tumor cells. We also investigated the expression pattern for oncogenesis-related genes in 789 genes using the Panther or GO function (Table 3). Oncogenesis-related genes were divided into three groups in different type. Normal letters were allocated from the Panther and GO process for function in oncogenesis; bold letters were allocated from Panther, GO process and journals, which have been published as both function progression and suppression in oncogenesis; and italic letters were allocated from Panther, GO process and journals, which have not been published as both function progression and suppression in oncogenesis (Table 3), showing that GC seems to induce gene expression to apoptosis and suppression of tumor (Fig. 5).

Discussion

In this study, the microarray data show that 789 transcripts were affected by our treatments (approximately 2.4% of the genome, FC > 1.5), representing a small percentage of the genes expressed in HEK293T cells. Furthermore, only 257 genes (approximately 0.8% of the genome, FC > 1.5) were highly upregulated in cells treated with PMA and significantly downregulated in cells treated with both GC and PMA. Flavonoids are natural polyphenols, which are widely distributed in many plants, and they produce antiallergic, antiinflammatory, antimicrobial, and anticancer activity [17]. They have previously been reported to inhibit the transcription factor NF-κB and the expression of NF-κB-regulated genes [18]. A subgroup of flavonoids flavan-3-ols [(−)-epicatechin and (+)-catechin] and a B dimeric procyanidin also inhibit PMA-induced NF-κB activation at multiple steps in Jurkat T cells [19].

NF-κB comprises a family of inducible transcription factors that serve as key regulators of the host's immune and inflammatory response system. Consistent with these roles is the fact that incorrect NF-κB regulation has been linked to cancer, inflammatory, and autoimmune diseases, septic shock, viral infection, and improper immune system development. In addition, stimulation of the NF-κB pathway is mediated by diverse signal transduction cascades. We investigated the inhibition of PMA-induced NF-κB-dependent transcriptional activity by a subgroup of flavonoids GC. GC (10 μg/ml) inhibited the PMA-induced NF-κB-dependent transcriptional activity in the HEK293T cells. The present microarray data indicate that GC highly modulated inflammation-related genes to inhibit inflammation, including immunity and defense-related genes, by modulating NF-κB-dependent pathways.

It seems that GC induces apoptosis through upregulation of all apoptosis-induction genes. Many flavonoids produce potent antitumor activity through induction of apoptosis and cell cycle arrest in several cancer cell lines. For example, a citrus flavone tangeretin induces apoptosis in human promyelocytic leukemia (HL-60) cells [7] and blocks cell cycle progression at the G1 phase in human colorectal carcinoma COLO 205 cells [6]. GC is also expected to act on apoptosis at cell cycle arrest through a group of genes. Our data for YARS relating to the induction of apoptosis matches previous results, which strongly suggests that the gene might contribute to the induction of apoptosis [20]. LIF is well known for its role in inducing of apoptosis: apoptosis induced by LIF is largely determined by target cell type and signal pathways

Fig. 3

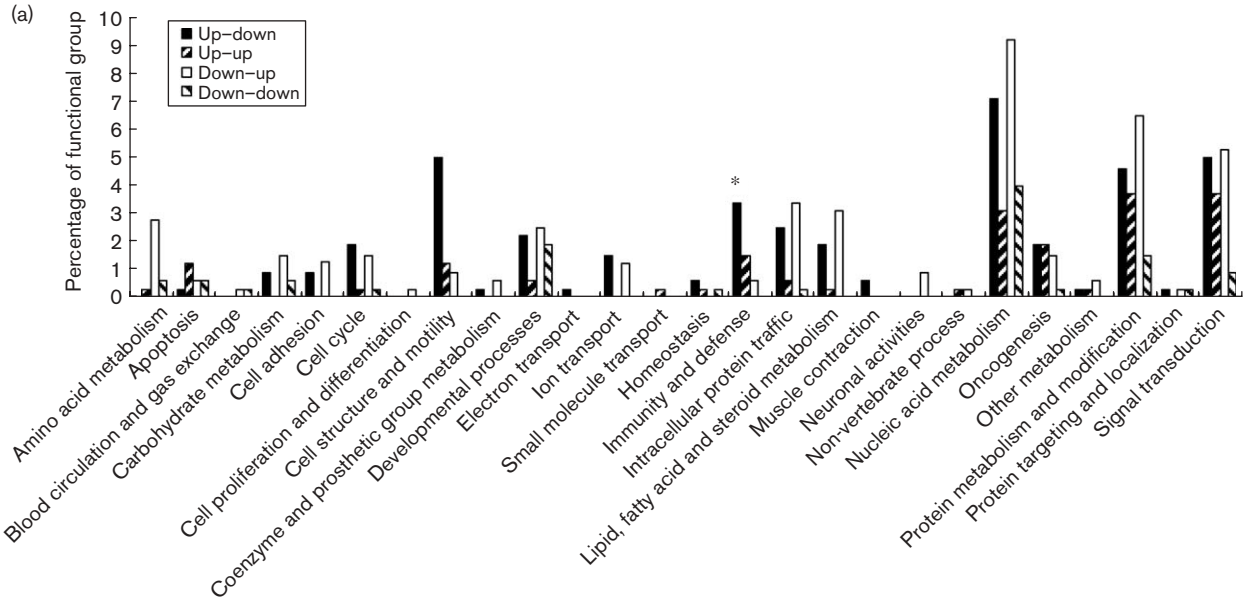

(b)

Gene symbol	Fold change		
	Gly	PMA	Gly+PMA
NF-κB1	1.7	8.9	5.3
CCL7	–7.6	8.3	4.3
CCL2	–5.2	4.8	3.0
HSPB8	–1.7	19.0	9.0
CD44	–6.1	5.4	1.4

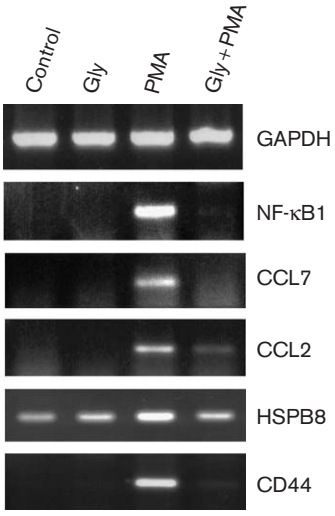

(c) I-κB degradation

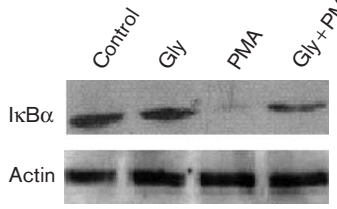

(d)

Gene symbol	Fold change		
	Gly	PMA	Gly+PMA
TIMP1	15.7	125.7	79.2

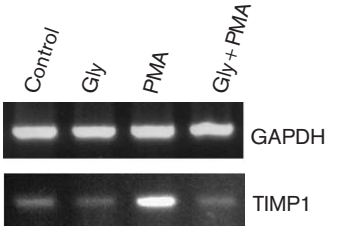

Expression manner of glycyrol-dependent genes. These results were obtained from three independent experiments on microarray chips. (a) A cluster was annotated to a functional group with four sets in Fig. 2c. (b) RT-PCR for microarray data. Glycyrol-dependent inhibition against induction of nuclear factor-κB gene and inflammation-related genes by phorbol 12-myristate 13-acetate (PMA). (c) Western blot pattern of glycyrol-dependent I-κBα based on microarray data. (d) RT-PCR result according to microarray data showed that TIMP1 having apoptosis inhibition effect was downregulated by glycyrol.

[21,22]. Meanwhile, p53, BID, and GZM-M were upregulated but CASPs (caspase 3, 6 and 7) were downregulated by GC. Among end-stage apoptotic nucleases, CAD/DFF B and AIF/PDCD8 were downregulated, but ENDO G was upregulated by GC. Biochemical and genetic studies have identified at least

Table 1 Inflammation-related genes screened from 789 genes (Fig. 2c) using the Panther process

Gene name	Genesymbol	Gene ID	Gly/control	PMA/control	PMA + glycyrol/ control
Genes upregulated by PMA, which are downregulated by glycyrol (set 1, up–down)					
Adenosine A2b receptor	ADORA2B	hCG28935.2	−1.34	1.57	1.36
β-2-microglobulin	B2M	hCG1786707.4	1.18	1.56	1.39
Chemokine (C-C motif) ligand 2	CCL2	hCG29298.3	−5.21	4.88	3.06
Chemokine (C-C motif) ligand 7	CCL7	hCG29304.2	−7.65	8.30	4.32
CD44 antigen (homing function and Indian blood group system)	CD44	hCG1811182.2	−6.11	5.43	1.42
CD59 antigen p18-20 (antigen identified by monoclonal antibodies 16.3A5, EJ16, EJ30, EL32, and G344)	CD59	hCG2033390	−1.18	2.07	1.83
CD83 antigen (activated B lymphocytes, immunoglobulin superfamily)	CD83	hCG36755.3	−1.54	2.58	1.97
Heat shock 22-kDa protein 8	HSPB8	hCG27207.2	−1.78	19.13	9.57
Interleukin 12A (natural killer cell stimulatory factor 1, cytotoxic lymphocyte maturation factor 1, p35)	IL12A	hCG1685939.3	2.37	5.75	4.34
Nuclear factor of κ light polypeptide gene enhancer in B cells 1 (p105)	NFKB1	hCG39336.2	1.75	8.95	5.31
Tumor necrosis factor (ligand) superfamily, member 9	TNFSF9	hCG23042.3	−1.82	1.63	−1.06
Genes upregulated by PMA, which are rather upregulated by glycyrol (set 2, up–up)					
Decay-accelerating factor for complement (CD55, Cromer blood group system)	DAF	hCG22206.2	1.58	2.95	3.20
S100 calcium binding protein A4 (calcium protein, calvasculin, metastasin, murine placental homolog)	S100A4	hCG2039630	−3.26	−2.80	−2.16
Pentaxin-related gene, rapidly induced by interleukin -1-β	PTX3	hCG26914.2	−6.40	2.14	3.42
Tumor protein, translationally controlled 1	TPT1	hCG32792.2	−8.59	−4.21	−1.27
CD209 antigen	CD209	hCG22558.2	−1.81	−1.67	1.41
Genes downregulated by PMA, which are upregulated by glycyrol (set 3, down–up)					
Peptidylprolyl isomerase (cyclophilin)-like 3	PPIL3	hCG16559.2	1.16	−1.63	−1.32
Glutathione S-transferase M5	GSTM5	hCG40245.4	−3.55	−7.36	−2.01

PMA, phorbol 12-myristate 13-acetate.

Table 2 The apoptosis-related genes screened from 789 genes using the Panther and GO process

Genes symbol	Gene ID	Function in apoptosis	Glycyrol/control	PMA/control	PMA + glycyrol/control
Set 2: genes upregulated by PMA, which are further upregulated by glycyrol (up–up)					
INHBA	hCG17283.4	Induction	1.18	2.97	3.26
GADD45A	hCG21703.4	Induction	4.14	7.26	17.91
RIPK2	hCG23840.2	Induction	1.77	3.01	3.45
FEM1B	hCG40603.2	Induction	1.31	1.61	1.95
LIF	hCG41296.3	Induction[a]	−3.14	2.34	2.82
Set 3: genes downregulated by PMA, which are upregulated by glycyrol (down–up)					
YARS	hCG39689.2	Induction	14.28	2.91	5.36
NME3	hCG42692.2	Induction	2.15	−3.56	−2.41
MAPT	hCG27664.3	Induction	−1.82	−4.92	−4.24

FC of PMA to control >1.5 (789 genes) → FC of PMA/control to PMA + glycyrol/control $> \pm 0.5$ (20 genes). Only the genes in set 2 (five genes) and set 3 (three genes) were then selected from four sets (20 genes) because glycyrol repressed the genes in set 1 (11 genes) and set 4 (one gene).
FEM1B, fem-1 homolog b (*C. elegans*); GADD45A, growth arrest and DNA damage inducible, α; INHBA, inhibin, βA (activin A, activin AB-α polypeptide); LIF, leukemia-inhibitory factor (cholinergic differentiation factor); MAPT, microtubule-associated protein τ; NME3, nonmetastatic cells 3, protein expressed in; PDCD8, programmed cell death 8 (apoptosis-inducing factor); PMA, phorbol 12-myristate 13-acetate; RIPK2, receptor-interacting serine-threonine kinase 2; YARS, tyrosyl-tRNA synthetase.
[a]The apoptosis function of genes in sets 2 and 3 including LIF were mentioned from the Panther and GO process in AVADIS and LIF was as both induction and inhibition in those process. These results were obtained from three independent experiments on microarray chips.

three nucleases for end-stage DNA fragmentation during cell death: CAD/DFF, AIF/PDCD 8, and ENDO G [23–25]. In HEK293T cells, both a caspase-independent mechanism and a caspase-dependent pathway may operate as well [26]. p53 can promote neuronal cell death independently of caspase activity [27] and the BID gene is transcriptionally regulated by p53 [28,29]. BID releases ENDO G from mitochondria [30]. GZMs are BID-dependent or BID-independent [31], and GZM-K directly processes BID to release ENDO G, leading to mitochondria-dependent cell death by loss of mitochondrial transmembrane potential ($\Delta\Psi_m$) and mitochondrial swelling (the morphology change of mitochondria) [32]. GZM-M is most similar to GZM-K among GZMs (A, B, H, K, and M) in humans [33]. GZM-M-induced cell death is caspase-independent [34], and GZM M causes mitochondria swelling and loss of mitochondrial transmembrane potential [35]. CAD/DFF is a dimeric protein consisting of the DFF B (DFF40) and DFF A (DFF45) subunits. CAD/DFF B contains an endonuclease activity, and its synthesis and folding critically depend on CAD/DFF A. On induction of apoptosis, CAD/DFF A is cleaved by caspase-3. CAD/DFF B is then activated to cleave DNA into nucleosomal-sized fragments and to induce chromatin condensation [36,37]. Our microarray data for the caspases, however, showed they are downregulated by

Fig. 4

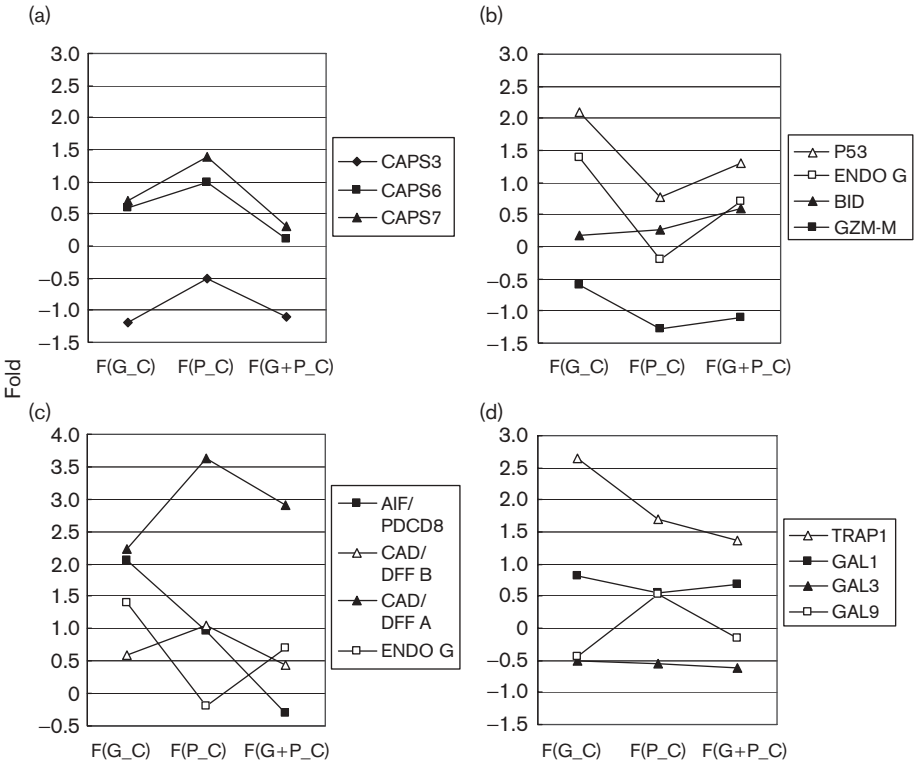

The downstream genes of apoptosis in HEK293T tumor cells modulated by glycyrol. These results were obtained from three independent experiments on microarray chips. (a) Downregulation of CASPs by glycyrol. (b) Upregulation of p53, ENDO G, BID, and GZM-M by glycyrol. (c) Downregulation of AIF/PDCD8, CAD/DFF A, and CAD/DFF B, and upregulation of ENDO G by glycyrol. (d) Upregulation of GAL1, and downregulation of GAL3, GAL9, and TRAP1 by glycyrol.

GC. Mitochondrial apoptogenic protein AIF/PDCD8 is released in response to apoptotic signals and translocates to the nucleus to induce DNA fragmentation and chromatin condensation in a caspase-independent manner [38]. It is, however, likely that AIF/PDCD8 is in a different pathway to that of ENDO G [39] by GC in HEK293T cells. This is why GC seems to induce the apoptosis-related genes using caspase-independent ENDO G instead of caspase-dependent CAD/DFF B or caspase-independent AIF/PDCD8 as downstream-apoptosis factor. Once released from mitochondria, ENDO G translocates to the nucleus during apoptosis and cleaves chromatin DNA into nucleosomal fragments, independently of caspases [30]. GAL1 were upregulated, but GAL3, GAL9, and TRAP1 (HSP75) were downregulated by GC. GAL1 induces nuclear tanslocation of ENDO G in caspase-independent and cytochrome *c*-independent T-cell death [40]. GAL3 expression, however, inhibits the loss of mitochondria membrane potential and GAL1 cell death is inhibited by GAL3 [40]. GAL9 has been shown to trigger death of various cell types via a caspase 1-dependent pathway [41]. TRAP1 acts as an antagonist and protects cells from GZM-M-mediated apoptosis [35]. These results show that GC seems to modulate the apoptosis-related genes, causing p53-dependent apoptosis using caspase-independent ENDO G as downstream apoptosis factor in HEK293T tumor cell lines, instead of caspase-dependent CAD/DFF B or caspase-independent AIF/PDCD8.

We had expected there to be a single direction of gene expression, that is, to tumor suppression through induction of apoptosis in HEK293T cells when treated with GC because all apoptosis-related genes that showed significant changes were for induction of apoptosis in the cells. In fact, a common mechanism of tumor suppression and induction of apoptosis exists [42]. Potentially, oncogenic proliferative signals are also coupled to a variety of growth-inhibitory processes, such as the induction of apoptosis [43], meaning that oncogenesis and apoptosis do not occur at the same time within the same cell lines because apoptosis plays an important role in maintaining normal tissue homeostasis [44]. NF-κB1 inhibits apoptosis through CDKN1A as shown in our result [1,45], induces cell proliferation, potentially blocks differentiation, and promotes metastasis [46]. FOS [47] and the

Table 3 The oncogenesis-related genes screened from 789 genes using the Panther and GO process

Genes symbol	Gene ID	Function in oncogenesis	Glycyrol/control	PMA/control	PMA + glycyrol/control
Set 1: genes upregulated by PMA, which are downregulated by glycyrol (up–down)					
MMP10	hCG41474.2	Progression	−8.96	4.75	4.28
DGKG	hCG2021087	Progression	1.33	8.95	8.42
STAT3	hCG1813145.1	Progression	1.54	2.62	1.52
SKI	Hcg23145.3	Progression	−3.37	−1.59	−2.73
ST7	**hCG15955.3**	**Progression**	**1.18**	**3.89**	**1.81**
LYN	hCG1810958.2	Progression	−2.52	1.94	−1.91
CD44	hCG1811182.2	Progression	−6.11	5.43	1.42
OGFR	Hcg1811182.3	Progression	−2.20	2.37	−3.69
CDKN1A	**hCG15367.4**	**Progression**	**3.84**	**27.45**	**14.16**
Set 2: genes upregulated by PMA, which are further upregulated by glycyrol (up–up)					
CTGF	**hCG22108.3**	**Suppression**	**1.33**	**23.78**	**68.02**
CYR61	**Hcg23652.3**	**Suppression**	**3.13**	**10.28**	**27.45**
TM4SF1	*hCG21217.3*	*Oncogenesis-related*	*−3.21*	*12.58*	*16.21*
SPANX	*hCG1756726.3*	*Oncogenesis-related*	*−8.72*	*6.13*	*9.31*
LMO2	hCG26502.3	Suppression	−6.38	−1.69	1.05
FOS	**hCG22355.3**	**Suppression**	**−24.91**	**1.82**	**3.80**
Set 3: genes downregulated by PMA, which are upregulated by glycyrol (down–up)					
EIF4EBP1	hCG23101.4	Suppression	21.03	2.96	8.16
CD99L2	hCG39239.3	Suppression	7.93	1.83	3.05
MTCP1	*HCG1640796.3*	*Oncogenesis-related*	*1.04*	*−2.13*	*−1.47*
MST1	**hCG2001992**	**Suppression**	**3.85**	**−1.62**	**−1.08**
ARMCX3	hCG20396.3	Suppression	1.09	−1.81	−1.34
Set 4: genes downregulated by PMA, which are further downregulated by Glycyrol (down-down)					
MN1	hCG40087.2	Progression	−1.65	−4.42	−12.27

FC of PMA to control >1.5 (789 genes) $\rightarrow$ FC of PMA/control to PMA + glycyrol/control $> \pm 0.5$ (21 genes). These results were obtained from three independent experiments on microarray chips. Normal letters were from Panther and GO process, bold letters from Panther, GO process and journals published as both function progression and suppression in oncogenesis, and italic letters from Panther, GO process and journals, still not published as both function progression and suppression in oncogenesis.

ARMCX3, armadillo repeat containing, X-linked 3; CD99L2, CD99 antigen-like 2; CTGF, connective tissue growth factor; CYR61, cysteine-rich, angiogenic inducer, 61; DGKG, diacylglycerol kinase, γ 90 kDa; EIF4EBP1, eukaryotic translation initiation factor 4E-binding protein 1; ETV5, ets variant gene 5 (ets-related molecule); FOS, v-fos FBJ murine osteosarcoma viral oncogene homolog; LMO2, LIM domain only 2 (rhombotin-like 1); LYN, v-yes-1 Yamaguchi sarcoma viral-related oncogene homolog; MMP10, matrix metalloproteinase 10 (stromelysin 2); MN1, meningioma (disrupted in balanced translocation) 1; MST1, macrophage stimulating 1 (hepatocyte growth factor-like); MTCP1, mature T cell proliferation 1; OGFR, opioid growth factor receptor; PMA, phorbol 12-myristate 13-acetate; SKI, v-ski sarcoma viral oncogene homolog (avian); SPANX, sperm protein associated with the nucleus, X-linked, family; ST7, suppression of tumorigenicity 7; TM4SF1, transmembrane-4 superfamily member 1.

CCN family (such as CTGF [48,49] and Cyr61 [50]) have a known role in tumor suppression. ST7 may have functions like tumor progressors because it also function as an oncogene in oral tumors [16], whereas MST1 has been identified as a putative tumor suppressor gene that binds to CDK4 and CDK6 (cyclin-dependent kinases), preventing their interaction with cyclin D1 and thereby preventing cell cycle progression at the G_1 stage [51]. SPANX genes encode testes cancer-specific antigens. Some of the SPANX family is, however, likely to be associated with susceptibility to certain cancers [52]. This family of genes tended to be induced as tumor suppressors by GC in this study. MTCP1 and TM4SF1 are thought to normally form part of a network of oncogenes and tumor suppressor genes because MTCP1 type B transcript was not observed in T cell prolyphocytic leukemia, though MTCP1 type A transcript was observed in the same cells [53]. CD9, CD82, CD63, and TM4SF1 belong to the transmembrane-4 superfamily (TM4SF) in which members CD9, CD82, and CD63 (except TM4SF1) are tumor supressors. Specifically, a splice variant of CD82 plays a role in tumor invasion and progression by removing exon 7 of the eight exons [54,55]. In Table 3, normal letters were allocated from Panther and GO processes for functions in oncogenesis; bold letters (ST7, CDKN1A, CTGF, CYR61, FOS) from Panther, GO process and journals, which have been published as both progression and suppression functions in oncogenesis; and italic letters (TM4SF1, SPANX, MTCP1) from Panther, GO process and journals, which have not been published as both progression and suppression function in oncogenesis. Our data thus show that TM4SF1, SPANX, and MTCP1 may have an added function of suppression in addition to their known function of progression in oncogenesis.

Predictions concerning disease detection and therapy can be made based on new information on biological expression. It is likely that GC represses inflammatory-related genes, induces apoptosis-related genes through p53-dependent pathway, and has a function for suppression of oncogenesis-related genes through phorbol ester-induced, NF-κB-dependent pathway. Therefore, GC may be linked to the inhibition of inflammation and to suppression of oncogenesis through p53-dependent apoptosis using ENDO G in the HEK293T tumor cell line, instead of CAD/DFF B or AIF/PDCD8 among the three known downstream-apoptosis factors. On the basis of these results, the GC expression profiling data showed changes of gene expression displaying with a unique signature from HEK293T cells and shared with inflammation, apoptosis, and oncogenesis, suggesting that GC may be a novel candidate for tumor suppressor.

Fig. 5

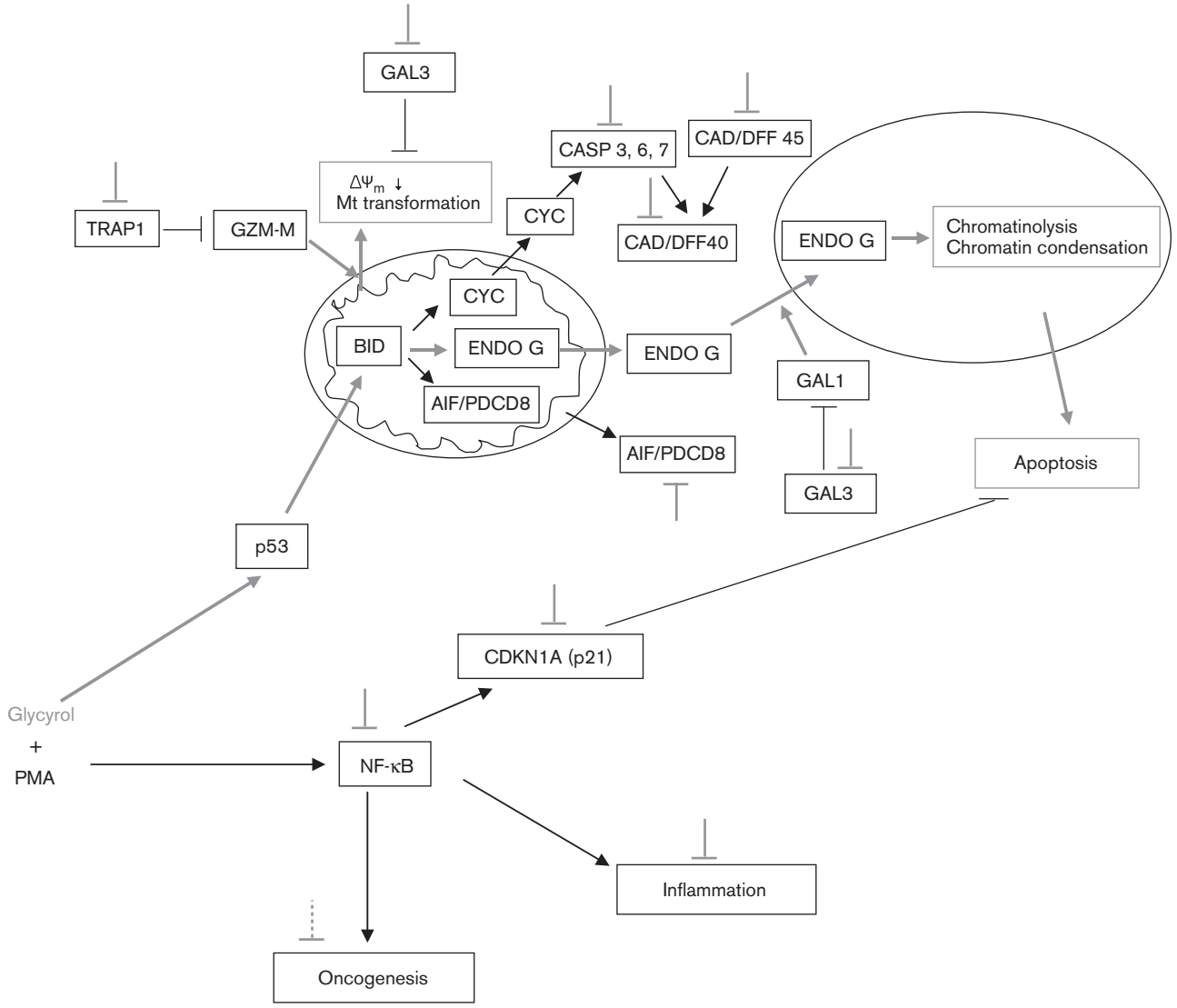

The putative modulation pathway by glycyrol in HEK293T tumor cells including an end stage of apoptosis. These results were obtained from three independent experiments on microarray chips. PMA-induced nuclear factor-κB-dependent pathway was shown in thin black. Glycyrol-induced pathway including p53-dependent pathway was shown in thick pink and repression by glycyrol was indicated as thick pink bar. The dotted line indicates predicted function. $\Delta\Psi_m$, mitochondrial potential; Mt, mitochondria.

Acknowledgements

This work was supported by the Korea Research Foundation Grant funded from the Korean Government (2006-E00286) and by the 2nd Stage of Brain Korea 21 (SungGa Lee and Won-Bong Lim).

References

1 Tak PP, Firestein GS. NF-κB: a key role in inflammatory diseases. *J Clin Invest* 2001; **107**:7–11.
2 Collins T, Cybulsky MI. NF-κB: pivotal mediator or innocent bystander in atherogenesis? *J Clin Invest* 2001; **107**:255–264.
3 Holmes-McNary M, Baldwin AS Jr. Chemopreventive properties of *trans*-resveratrol are associated with inhibition of activation of the IκB kinase. *Cancer Res* 2000; **60**:3477–3483.
4 Huang C, Ma W, Goranson A, Dong Z. Resveratrol suppresses cell transformation and induces apoptosis through a p53-dependent pathway. *Carcinogenesis* 1999; **20**:237–242.
5 Wenzel U, Kuntz S, Brendel MD, Daniel H. Dietary flavone is a potent apoptosis inducer in human colon carcinoma cells. *Cancer Res* 2000; **60**:3823–3831.
6 Pan MH, Chen WJ, Lin-Shiau SY, Ho CT, Lin JK. Tangeretin induces cell-cycle G1 arrest through inhibiting cyclin-dependent kinases 2 and 4 activities as well as elevating Cdk inhibitors p21 and p27 in human colorectal carcinoma cells. *Carcinogenesis* 2002; **23**:1677–1684.
7 Hirano T, Abe K, Gotoh M, Oka K. Citrus flavone tangeretin inhibits leukaemic HL-60 cell growth partially through induction of apoptosis with less cytotoxicity on normal lymphocytes. *Br J Cancer* 1995; **72**:1380–1388.
8 Saitoh T, Shibata S. Chemical studies on the oriental plant drugs. XXII. Some new constituents of licorice root. Glycyrol, 5-*O*-methylglycyrol and isoglycyrol. *Chem Pharm Bull (Tokyo)* 1969; **17**:729–734.

9 Wang CL, Zhang RY, Han YS, Dong XG, Liu WB. Chemical studies of coumarins from *Glycyrrhiza uralensis* Fisch. *Yao Xue Xue Bao* 1991; **26**:147–151.

10 Yang L, Liu YL, Lin SQ. HPLC analysis of flavonoids in the root of six *Glycyrrhiza* species. *Yao Xue Xue Bao* 1990; **25**:840–848.

11 Shim SB, Kim NJ, Kim DH. Beta-glucuronidase inhibitory activity and hepatoprotective effect of 18 beta-glycyrrhetinic acid from the rhizomes of *Glycyrrhiza uralensis*. *Planta Med* 2000; **66**:40–43.

12 Kondratenko RM, Baltina LA, Vasil'eva EV, Ismagilova AF, Nasyrov Kh M, Baschenko N, *et al*. Synthesis and immunostimulating activity of cysteine-containing glycopeptide derivatives of glycyrrhizic acid. *Bioorg Khim* 2004; **30**:61–67.

13 Kondratenko RM, Baltina LA, Vasil'eva EV, Nasyrov Kh M, Kireeva RM, Baschenko N, *et al*. Synthesis and immunomodulating activity of new diglycopeptides of glycyrrhizinic acid and its 30-methyl ester. *Bioorg Khim* 2004; **30**:168–173.

14 Kondratenko RM, Baltina LA, Mustafina SR, Vasil'eva EV, Pompei R, Deidda D, *et al*. The synthesis and antiviral activity of glycyrrhizic acid conjugates with alpha-D-glucosamine and some glycosylamines. *Bioorg Khim* 2004; **30**:308–315.

15 Kondratenko RM, Mustafina SR, Baltina LA, Vasil'eva NG, Ismagilova AF, Vasil'eva EV, *et al*. Synthesis and antiulcer activity of 3-*O*-acylated glycyrrhetic acid methylates. *Pharmaceutic Chem J* 2001; **35**:243–246.

16 Li G, Fridman R, Choi Kim HR. Tissue inhibitor of metalloproteinase-1 inhibits apoptosis of human breast epithelial cells. *Cancer Res* 1999; **59**:6267–6275.

17 Yamamoto Y, Gaynor RB. Therapeutic potential of inhibition of the NF-κB pathway in the treatment of inflammation and cancer. *J Clin Invest* 2001; **107**:135–142.

18 Saliou C, Valacchi G, Rimbach G. Assessing bioflavonoids as regulators of NF-κB activity and inflammatory gene expression in mammalian cells. *Methods Enzymol* 2001; **335**:380–387.

19 Mackenzie GG, Carrasquedo F, Delfino JM, Keen CL, Fraga CG, Oteiza PI. Epicatechin, catechin, and dimeric procyanidins inhibit PMA-induced NF-κB activation at multiple steps in Jurket T cells. *FASEB J* 2004; **18**:167–169.

20 Wakasugi K, Schimmel P. Two distinct cytokines released from a human aminoacyl tRNA synthetase. *Science* 1999; **284**:147–151.

21 Kamohara H, Sakamoto K, Ishiko T, Masuda Y, Abe T, Ogawa M. Leukemia inhibitory factor induces apoptosis and proliferation of human carcinoma cells through different oncogene pathways. *Int J Cancer* 1997; **72**: 687–695.

22 Lu Y, Fukuyama S, Yoshida R, Kobayashi T, Saeki K, Shiraishi H, *et al*. Loss of SOCS3 gene expression converts STAT3 function from anti-apoptotic to pro-apoptotic. *J Biol Chem* 2006; **281**:36683–36690.

23 Schindler CK, Pearson EG, Bonner HP, So NK, Simon RP, Prehn JHM, *et al*. Caspase-3 cleavage and nuclear localization of caspase-activated DNase in human temporal lobe epilepsy. *J Cereb Blood Flow Metab* 2006; **26**:583–589.

24 Chiarugi A. Simple but not simpler: toward a unified picture of energy requirements in cell death. *FASEB J* 2005; **19**:1783–1788.

25 Jaeschke H, Bajt ML. Intracellular signaling mechanisms of acetaminophen-induced liver cell death. *Toxicol Sci* 2006; **89**:31–41.

26 Livne A, Shtrichman R, Kleinberger T. Caspase activation by adenovirus E4orf4 protein is cell line specific and is mediated by the death receptor pathway. *J Virol* 2001; **75**:789–798.

27 Johnson MD, Kinoshita Y, Xiang H, Ghatan S, Morrison RS. Contribution of p53-dependent caspase activation to neuronal cell death declines with neuronal maturation. *J Neurosci* 1999; **19**:2996–3006.

28 Sax JK, Fei P, Murphy ME, Bernhard E, Korsmeyer SJ, El-Deiry WS. BID regulation by p53 contributes to chemosensitivity. *Nat Cell Biol* 2002; **4**:842–849.

29 Haupt S, Berger M, Goldberg Z, Haupt Y. Apoptosis – the p53 network. *J Cell Sci* 2003; **116**:4077–4085.

30 Li LY, Luo X, Wang X. Endonuclease G is an apoptotic DNase when released from mitochondria. *Nature* 2001; **412**: 95–99.

31 Galluzzi L, Maiuri MC, Vitale I, Zischka H, Castedo M, Zitvogel L, *et al*. Cell death modalities: classification and pathophysiological implications. *Cell Death Differ* 2007; **14**:1237–1243.

32 Zhao T, Zhang H, Guo Y, Fan Z. Granzyme K directly processes Bid to release cytochrome C and endonuclease G leading to mitochondria-dependent cell death. *J Biol Chem* 2007; **282**:12104–12111.

33 Grossman WJ, Revell PA, Lu ZH, Johnson H, Bredemeyer AJ, Ley TJ. The orphan granzymes of humans and mice. *Curr Opin Immunol* 2003; **15**:544–552.

34 Kelly JM, Waterhouse NJ, Cretney E, Browne KA, Ellis S, Trapani JA, *et al*. Granzyme M mediates a novel form of perforin-dependet cell death. *J Biol Chem* 2004; **279**:22236–22242.

35 Hua G, Zhang Q, Fan Z. Heat shock protein 75 (TRAP1) antagonizes reactive oxygen species generation and protects cells from granzyme M-mediated apoptosis. *J Biol Chem* 2007; **282**:20553–20560.

36 Zhang J, Dong M, Li L, Fan Y, Pathre P, Dong J, *et al*. Endonuclease G is required for early embryogenesis and normal apoptosis in mice. *Proc Natl Acad Sci USA* 2003; **100**:15782–15787.

37 Widlak P, Garrard WT. Discovery, regulation, and action of the major apoptotic nucleases DFF40/CAD and endonuclease G. *J Cell Biochem* 2005; **94**:1078–1087.

38 Susin SA, Lorenzo HK, Zamzami N, Marzo I, Snow BE, Bro'thers GM, *et al*. Molecular characterization of mitochondrial apoptosis-inducing factor. *Nature* 1999; **397**:441–446.

39 Liu T, Biddle D, Hanks AN, Brouha B, Yan H, Lee RM, *et al*. Activation of dual apoptotic pathways in human melanocytes and protection by survivin. *J Invest Dermatol* 2006; **126**:2247–2256.

40 Hahn HP, Pang M, He J, Hernandez JD, Yang RY, Li LY, *et al*. Galectin-1 induces nuclear translocation of endonuclease G in caspase- and cytochrome c-independent T cell death. *Cell Death Differ* 2004; **11**: 1277–1286.

41 Kashio Y, Nakamura K, Abedin MJ, Seki M, Nishi N, Yoshida N, *et al*. Galectin-9 induces apoptosis through the calcium-calpain-caspase-1 pathway. *J Immunol* 2003; **170**:3631–3636.

42 Roperch JP, Lethrone F, Prieur S, Piouffre L, Israeli D, Tuynder M, *et al*. SIAH-1 promotes apoptosis and tumor suppression through a network involving the regulation of protein folding, unfolding, and trafficking: identification of common effectors with p53 and $p21^{Waf1}$. *Proc Natl Acad Sci USA* 1999; **96**:8070–8073.

43 Evan GI, Vousden KH. Proliferation, cell cycle and apoptosis in cancer. *Nature* 2001; **411**:342–348.

44 Deng J, Xia W, Hung MC. Adenovirus 5 E1A-mediated tumor suppression associated with E1A-mediated apoptosis *in vivo*. *Oncogene* 1998; **17**:2167–2175.

45 Gartel AL, Tyner AL. The role of the cyclin-dependent kinase inhibitor p21 in apoptosis. *Mol Cancer Ther* 2002; **1**:639–649.

46 Baldwin AS. Control of oncogenesis and cancer therapy resistance by the transcription factor NF-κB. *J Clin Invest* 2001; **107**:241–246.

47 Fleischmann A, Jochum W, Eferl R, Witowsky J, Wagner EF. Rhabdomyosarcoma development in mice lacking Trp53 and Fos: tumor suppression by the Fos protooncogene. *Cancer Cell* 2003; **4**:477–482.

48 Hishikawa K, Oemar BS, Tanner FC, Nakaki T, Lüscher TF, Fujii T. Connective tissue growth factor induces apoptosis in human breast cancer cell line MCF-7. *J Biol Chem* 1999; **274**:37461–37466.

49 Moritani NH, Kubota S, Nishida T, Kawaki H, Kondo S, Sugahara T, *et al*. Suppressive effect of overexpressed connective tissue growth factor on tumor cell growth in a human oral squamous cell carcinoma-derived cell line. *Cancer Lett* 2003; **192**:205–214.

50 Tong X, Xie D, O'Kelly J, Miller CW, Muller-Tidow C, Koeffler HP. Cyr61, a member of CCN family, is a tumor suppressor in non-small cell lung cancer. *J Biol Chem* 2001; **276**:47709–47714.

51 Shigemasa K, Hu C, West CM, Clarke J, Parham GP, Parmley TH, *et al*. p16 overexpression: a potential early indicator of transformation in ovarian carcinoma. *J Soc Gynecol Investig* 1997; **4**:95–102.

52 Kouprina N, Noskov VN, Solomon G, Otstot J, Isaacs W, Xu J, *et al*. Mutational analysis of SPANX genes in families with X-linked prostate cancer. *Prostate* 2007; **67**:820–828.

53 Chun HH, Castellvi-Bel S, Wang Z, Nagourney RA, Plaeger S, Becker-Catania SG, *et al*. TCL-1, MTCP-1 and TML-1 gene expression profile in non-leukemic clonal proliferations associated with ataxia-telangiectasia. *Int J Cancer* 2002; **97**:726–731.

54 Miyake M, Inufusa H, Adachi M, Ishida H, Hashida H, Tokuhara T, *et al*. Suppression of pulmonary metastasis using adenovirally motility related protein-1 (MRP-1/CD9) gene delivery. *Oncogene* 2000; **19**:5221–5226.

55 Lee JH, Seo YW, Park SR, Kim YJ, Kim KK. Expression of a splice variant of KAI1, a tumor metastasis suppressor gene, influences tumor invasion and progression. *Cancer Res* 2003; **63**:7247–7255.